Available online at www.sciencedirect.com
SCIENCE DIRECT®
Atmospheric Environment 39 (2005) 1765–1774
ATMOSPHERIC ENVIRONMENT
www.elsevier.com/locate/atmosenv

Measurements of the kinetics of the OH-initiated oxidation of α-pinene: Radical propagation in the OH + α-pinene + O_2 + NO reaction system

Maxine E. Davis, Philip S. Stevens*

Department of Chemistry and Environmental Science Research Center, School of Public and Environmental Affairs, Indiana University, Bloomington, IN 47405, USA

Received 28 January 2004; accepted 28 September 2004

Abstract

The mechanism of the OH-initiated oxidation of α-pinene in the presence of NO has been investigated using a discharge-flow system at 5 Torr and 300 K. The OH concentration was monitored as a function of reaction time by laser-induced fluorescence (LIF). The rate constant for the OH + α-pinene was measured to be $(6.09 \pm 0.30) \times 10^{-11}$ cm^3 $molecule^{-1}$ s^{-1}. OH radical regeneration was observed after addition of O_2 and NO, and the measured OH concentration profiles were compared to simulations based on both the Master Chemical Mechanism and the Regional Atmospheric Chemistry Mechanism for α-pinene oxidation in order to determine the ability of these mechanisms to describe the observed efficiency of radical propagation. Both models are able to reproduce the observed OH concentrations profiles to within 30%. However, expanding the MCM to include isomerization of the β-hydroxy alkoxy radicals improves the agreement with the experimental observations.

Keywords: α-pinene; Hydroxyl radical; Tropospheric chemistry; Kinetics; Mechanism

1. Introduction

The emission of natural hydrocarbons is an important source of volatile organic compounds (VOCs) to the atmosphere. Between 800 and 1200 Tg of biogenic VOCs have been estimated to be emitted globally each year (Guenther et al., 1995) compared to 100 Tg of anthropogenic hydrocarbons. Because of their high reactivities, biogenic VOCs can have a great impact on both regional and global air quality. The most abundant natural volatile organic compounds emitted by vegetation are isoprene and the monoterpenes. Globally, monoterpenes make up 10% of the biogenic hydrocarbons emitted yearly, with α-pinene and β-pinene being the most abundant of these emitted in North America (Guenther et al., 2000).

α-Pinene is removed from the atmosphere by its reaction with the OH radical, O_3 and the NO_3 radical (Atkinson, 2000). During the day, the reaction with OH radical dominates while that with O_3 and NO_3 are significant at night (Atkinson and Arey, 1998, 2003). Because of its high reactivity with the OH radical, emissions of α-pinene can contribute significantly to ozone and secondary aerosol formation in the troposphere. A thorough understanding of the OH-initiated oxidation of α-pinene, particularly in the presence of

*Corresponding author. Tel.: +1 812 855 0732; fax: +1 812 855 7802.
E-mail address: pstevens@indiana.edu (P.S. Stevens).

1352-2310/$ - see front matter © 2004 Elsevier Ltd. All rights reserved.
doi:10.1016/j.atmosenv.2004.09.068

NO_x (= NO + NO_2) is thus important for the development of effective air quality control strategies. Recent measurements of OH and HO_2 in the troposphere have shown that there are serious discrepancies between measured and modeled concentrations of HO_x, which question our understanding of the complex radical chemistry of the lower troposphere.

The mechanism for the OH-initiated oxidation of α-pinene is thought to begin with the addition of OH to the double bond to form β-hydroxy alkyl radicals (Aschmann et al., 2002; Atkinson, 1994; Atkinson, 1997; Atkinson et al., 1999). The subsequent addition of an oxygen molecule leads to the formation of peroxy radicals (RO_2), and reactions of these peroxy radicals with NO lead to the formation of NO_2, hydroperoxy radicals (HO_2), and a variety of products including organic nitrates ($RONO_2$), pinonaldehyde, acetone, and various carbonyls. Measured yields of pinonaldehyde between 28% and 87% have been reported (Arey et al., 1990; Aschmann et al., 2002; Hakola et al., 1994; Hatakeyama et al., 1991; Larsen et al., 2001; Noziere et al., 1999; Wisthaler et al., 2001). The higher pinonaldehyde values have been those obtained by FTIR, while GC–FID and PTR–MS have produced lower values. It has been suggested that the high measurements by FTIR is due to interferences from other carbonyl compounds or incorrect calibration of the IR absorption bands of pinonaldehyde (Aschmann et al., 2002). Measured yields of acetone are in better agreement, with reported yields between 5% and 11% (Noziere et al., 1999; Orlando et al., 2000; Larsen et al., 2001; Wisthaler et al., 2001), and measured total organic nitrates yields between 1% and 18% have been reported (Noziere et al., 1999; Aschmann et al., 2002).

Recently, several different complete and partial reaction schemes have been suggested (Aschmann et al., 2002; Atkinson and Arey, 1998; Dibble, 2001; Noziere et al., 1999; Orlando et al., 2000; Peeters et al., 2001). Common to several of these schemes is the prompt formation of pinonaldehyde with HO_2 production, with formation of additional carbonyl compounds from 1,5 H-shift or 1,6 H-shift isomerizations and decompositions. A general outline of the mechanism is given below:

$$RH + OH \rightarrow R, \quad \text{(R1)}$$

$$R + O_2 \rightarrow RO_2, \quad \text{(R2)}$$

$$RO_2 + NO \rightarrow RONO_2, \quad \text{(R3)}$$

$$RO_2 + NO \rightarrow RO + NO_2, \quad \text{(R4)}$$

$$RO(+O_2) \rightarrow \text{products} + HO_2 \rightarrow O_2 \text{ reaction/decomposition}, \quad \text{(R5a)}$$

$$RO \rightarrow R' \text{ isomerization}, \quad \text{(R5b)}$$

$$HO_2 + NO \rightarrow OH + NO_2, \quad \text{(R6)}$$

$$NO_2 + h\nu \rightarrow O + NO, \quad \text{(R7)}$$

$$O + O_2 \rightarrow O_3. \quad \text{(R8)}$$

Similar to the OH-initiated oxidation of other volatile organic compounds, the OH-initiated oxidation of α-pinene produces a radical chain that cycles OH into peroxy radicals, which are then converted back to OH through reactions with NO (R1–R6). Recent measurements of OH and HO_2 in the atmosphere have shown that there are serious discrepancies between measured and modeled concentrations of HO_x in the lower troposphere, with observed OH levels lower than modeled concentrations by as much as 50% (Carslaw et al., 1999; George et al., 1999; McKeen et al., 1997; Stevens et al., 1997) although in a few cases (e.g. Tan, 2001) observed OH concentrations were higher than model predictions. These results bring into question our understanding of the complex radical chemistry of the lower troposphere, and the efficiency of radical cycling by various compounds.

This paper presents the results of measurements of the rate constant for the OH + α-pinene reaction at 300 K and 5 Torr and results of the measurements of the efficiency of OH radical propagation in the OH + α-pinene + O_2 + NO reaction system. The latter experiments are compared to predictions based on proposed mechanisms for the OH–initiated oxidation of α-pinene to evaluate the ability of these mechanisms to reproduce the observed OH radical concentrations, providing additional experimental data to help resolve the discrepancies between measured and modeled HO_x concentrations in the atmosphere.

2. Experimental methods

Experiments were done using the discharge-flow (DF) technique (Howard, 1979) using laser-induced fluorescence (LIF) detection of the OH radical. The experimental system is similar to those described elsewhere (Chuong and Stevens, 2000). The main body of the flow reactor is made of a 120 cm long, 25 mm internal diameter Pyrex glass tube coated with halocarbon wax (Halocarbon Corporation) to reduce the loss of radicals on the reactor walls. A movable injector (3 mm o.d.), also coated with halocarbon wax was used for the injection of α-pinene. The system was evacuated using Leybold D16B mechanical pump resulting in a bulk flow velocity of 10.1–11.0 m s^{-1} at 300 K. The system pressure was measured in the reaction zone using a MKS Baratron capacitance manometer.

Helium, used as the main carrier gas, was introduced into the system by a MKS flow controller. OH radicals were produced using the $F + H_2O \rightarrow OH + HF$ reaction ($k^{II} = 1.1 \times 10^{-11}$ cm^3 molecule^{-1} s^{-1}). A microwave generator (Opthos Instruments Inc.) was used to create a discharge to produce F atoms from a mixture of CF_4 in He. Water (approximately 5×10^{13} cm^{-3}) was added in excess 2 cm upstream of the radical port. Oxygen ($2–6 \times 10^{15}$ molecule cm^{-3}) was introduced to the reaction zone at a position 11.5 cm downstream of the fixed radical injection port.

OH radicals were detected by LIF using the frequency-doubled output of a 20 Hz Nd:YAG-pumped dye laser (Lambda Physik). Excitation of the OH radicals was done using the A–X (1,0) band via the Q(1) transition near 282 nm. The resulting A–X fluorescence near 308 nm was detected by a photomultiplier tube (Hamamatsu H5920-01) equipped with photon counting electronics at a right angle to the laser source. An interference filter centered at 308 nm (Esco Products) with a 10 nm bandpass and 20% transmission was fitted in front of the photomultiplier tube, and the detection system was gated to reject laser light scatter and background signals. The laser power was kept at 0.4 mW to reduce saturation of the OH absorption and the detector electronics. The system sensitivity was 1×10^{-8} counts s^{-1} cm^3 molecule^{-1} with a typical background count of 50 counts s^{-1}, resulting in a detection limit of 3×10^8 molecule cm^3 ($S/N = 1$, 10 s integration). The system was calibrated by titrating a known concentration of NO_2 in an excess of hydrogen atoms using the $H + NO_2 \rightarrow OH + NO$ reaction.

α-Pinene was purified by several freeze–pump–thaw cycles, and mixtures of ~0.3% were prepared by evaporating the purified α-pinene into a volume-calibrated 5.5 L reservoir fitted with a capacitance manometer and then diluting with He. Concentrations of α-pinene ($3.2–22.2 \times 10^{11}$ molecule cm^{-3}) were introduced into the reactor through the movable injector and determined by measuring the pressure drop in the calibrated volume over time. For the radical propagation experiments, NO was purified by passing through an ascarite trap and added through the moveable injector with a MKS flow controller.

Addition of α-pinene to the flow system increases loss of OH radicals to the walls of the reactor as preliminary pseudo-first-order decays of OH were non-linear. The loss is likely due to heterogeneous reactions of OH with α-pinene adsorbed onto the walls of the reactor. This was evidenced by the very slow recovery of the OH signal when the α-pinene flow was stopped at the end of each decay measurement. This behavior has been observed previously in the OH + isoprene (Chuong and Stevens, 2000; Stevens et al., 1999) and Cl + isoprene (Bedjanian et al., 1998; Stutz et al., 1998) reactions. This effect was reduced by conditioning the reactor with high concentrations of fluorine radicals, which may reduce the polarity of the walls by removing hydrogen atoms from the halocarbon wax coating (Chuong and Stevens, 2003). Addition of O_2 to the system may also inhibit these active sites on the walls.

Carbon tetraflouride (2% in He), and NO (99%) were obtained from Matheson Gas Products. Ultra high purity O_2 (99.999%), and Zero grade He (99.995%), were purchased from Indiana Oxygen. α-Pinene (99%) was obtained from Aldrich.

3. Results

To provide a benchmark for the OH + α-pinene + O_2 + NO radical propagation experiments, the rate constant for the OH + α-pinene reaction was measured at 300 K and 5 Torr. The conditions for the experiments are summarized in Table 1. Experiments were conducted under pseudo-first-order conditions with α-pinene concentration being in large excess of the OH concentrations. The observed pseudo-first-order decay (k^I_{obs}) was corrected for diffusion and OH loss on the movable injector (k_{inj}) as follows:

$$k^I_{obs} = k^I\left(1 + \frac{k^I D}{v^2}\right) - k_{inj}. \quad (1)$$

In this equation, D is the diffusion coefficient for OH and v (cm s^{-1}) is the bulk velocity.

The pseudo-first-order rate constant (k^I_{obs}, s^{-1}) was obtained from a weighed fit of a plot of the natural logarithm of the detected OH fluorescence signal versus reaction distance, which was converted to reaction time under the plug-flow approximation. A typical plot of the data is presented in Fig. 1. The corrected pseudo-first-order rate constants were plotted against the α-pinene concentration to obtain the second-order rate constant. Fig. 2 shows a plot of the results at 300 K. A weighted least-squares fit of the data in Fig. 2 gives a value of

Table 1
Summary of experimental conditions

Parameter	Value
α–Pinene concentration	$(0.3–2.2) \times 10^{12}$ molecule cm^{-3}
Temperature	300 K
Pressure range	5.0–5.4 Torr
Flow velocity	10.1–14.8 m s^{-1}
Carrier gas	He
OH concentration	$< 3 \times 10^{11}$ cm^{-3}
O_2 concentration	$(0.2–2.2) \times 10^{16}$ cm^{-3}
NO concentration	$(0–3) \times 10^{13}$ cm^{-3}
Diffusion coefficient	OH in He, $0.145T^{3/2}/P_{Torr}$ cm^2 s^{-1} (<5% correction)
First-order OH wall removal rates	< 10 s^{-1}

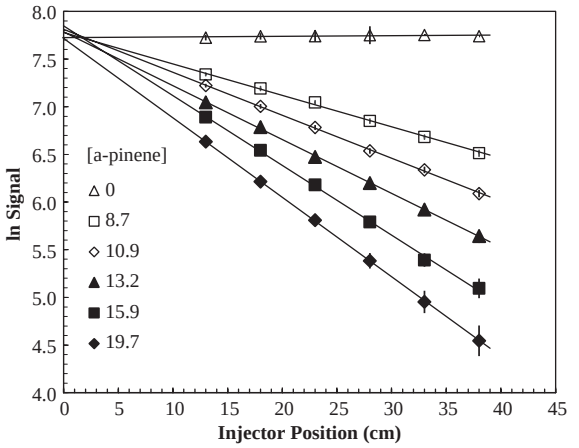

Fig. 1. Sample pseudo-first-order plot of the OH + α-pinene reaction at 5 Torr and 300 K. α-Pinene concentrations are in units of 10^{11} molecule cm^{-3}.

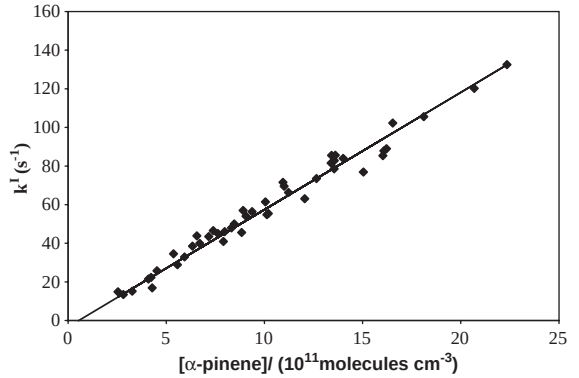

Fig. 2. Second-order plot for the OH + α-pinene reaction at 5 Torr and 300 K.

$(6.09 \pm 0.30) \times 10^{-11}$ cm^3 $molecule^{-1}$ s^{-1} for the OH + α-pinene rate constant at 5 Torr and 300 K, in excellent agreement with the value of $(6.08 \pm 0.24) \times 10^{-11}$ cm^3 $molecule^{-1}$ s^{-1} reported previously under similar conditions (Chuong et al., 2002). The error in the bimolecular rate constant represents two times the standard deviation from the weighted fit.

This result is in excellent agreement with the room temperature value of $(6.01 \pm 0.82) \times 10^{-11}$ cm^3 $molecule^{-1}$ s^{-1} measured by Kleindienst et al. (1982) using flash photolysis with resonance fluorescence at 50 Torr pressure, and in good agreement with the room temperature values of (5.45 ± 0.34) and $(5.78 \pm 0.86) \times 10^{-11}$ cm^3 $molecule^{-1}$ s^{-1} measured by Atkinson et al. (1986) and Winer et al. (1976), respectively, in synthetic air at 1 atm, and the value of $(5.05 \pm 1.23) \times 10^{-11}$ cm^3 $molecule^{-1}$ s^{-1} reported by Gill and Hites (2002) using relative rate methods.

With the addition of NO to the OH + α-pinene + O_2 reaction system at 300 K and 5 Torr, radical cycling was observed. The efficiency of this radical propagation was determined at various α-pinene concentrations by comparing the time evolution of the OH concentration profile in the absence of NO with the profile obtained when known concentrations of NO were added. The concentration of NO was kept below 3×10^{13} molecule cm^{-3} to ensure that radical propagation remained NO-limiting and to minimize OH radical loss due to the $RO + NO + M \rightarrow RONO + M$ and $OH + NO + M \rightarrow HONO + M$ reactions.

Computer simulations of the OH concentration profiles were done with the Kintecus Chemical simulator (Ianni and Bandy, 2000) using the Master Chemical Mechanism (MCM) as described by Saunders et al. (2003) for the oxidation of α-pinene. The MCM is a near-explicit chemical mechanism based on known reaction rates combined with structure–reactivity correlations. It describes the reaction pathways for the OH, O_3 and NO_3 initiated oxidation for several volatile organic compounds (VOCs) and the subsequent reaction of their oxidation products. The complete degradation mechanism for the α-pinene molecule was extracted from the primary VOC list and photolysis reactions were removed. Fig. 3 shows the important reaction in the presence of NO for α-pinene as outlined in the MCM mechanism depicted with bold arrows. In this reaction scheme OH is added to α-pinene in the C2 or C3 positions. For the C2 alkyl radical, both isomerization of the chemically activated adduct leading to ring breaking and reaction of the thermalized adduct with O_2 occur, with isomerization assumed to contribute with a 7.5% yield based on observed acetone yields (Noziere et al. 1999; Orlando et al., 2000; Larsen et al., 2001; Wisthaler et al., 2001) and as suggested by theoretical calculations (Vereecken and Peeters, 2000; Peeters et al., 2001). For the remaining alkyl radicals, reaction with molecular oxygen leads to the formation of β-hydroxy peroxy radicals which react with NO to form alkoxy radicals (77%) and organic nitrates (23%). Decomposition of the alkoxy radicals leads to the formation of pinonaldehyde and HO_2. The model also includes the subsequent oxidation of the intermediate products of the α-pinene oxidation such as pinonaldehyde, as well as self- and cross-reactions of the various peroxy radicals in the reaction mechanism. Except for OH + α-pinene, the rate constants used in this model were based on the recommended values as discussed by Saunders et al. (2003) and the important rates are listed in Table 2. The rate constant for the initial OH + α-pinene reaction as measured in this study was used in our simulations. The initial OH concentration used in the simulation was determined from the instrument calibration and adjusted to fit the observed OH decay in the

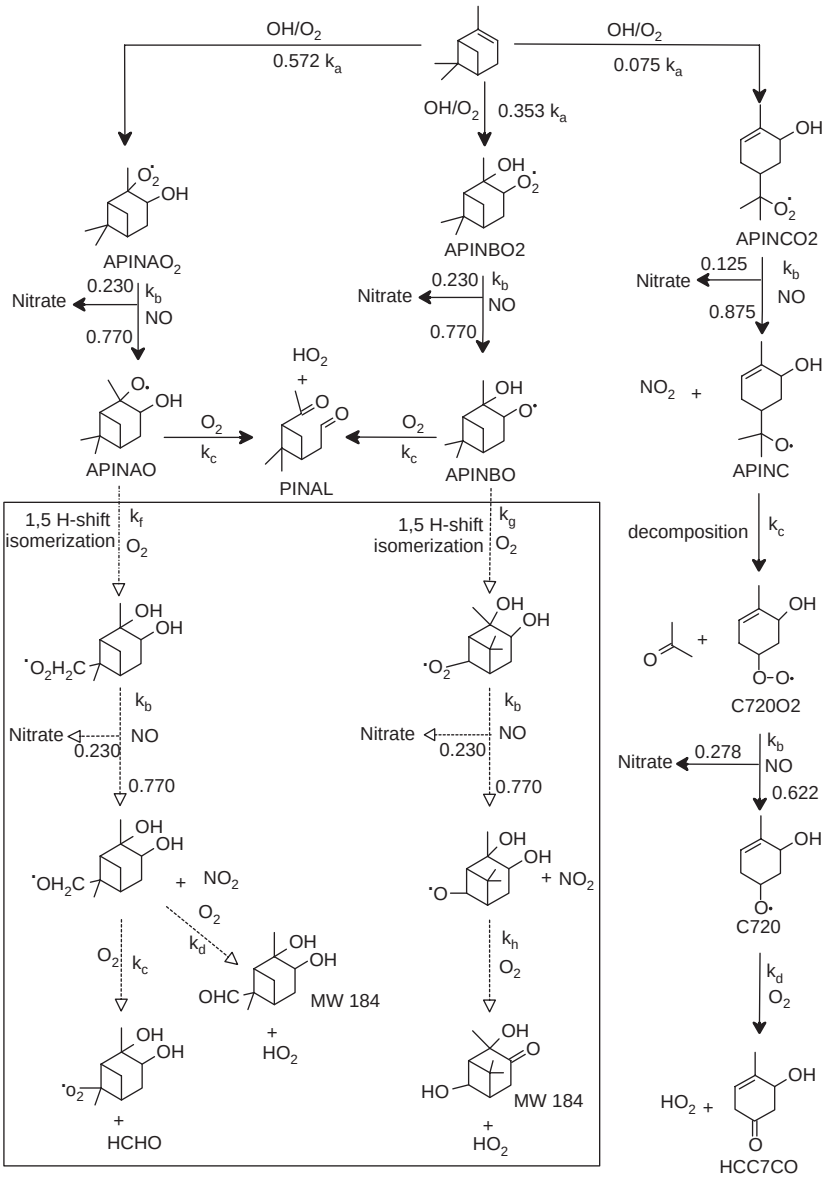

Fig. 3. Schematic mechanism for the OH-initiated oxidation of α-pinene. Rate constants are listed in Table 2. The bold arrows indicate the pathways included in the MCM scheme. Additional isomerization reactions are illustrated inside the box.

absence of NO, and this same OH concentration was used to simulate the OH concentration profiles in the presence of NO.

The results of four typical experiments are shown in Fig. 4. In this figure, the solid symbols are the measured OH concentrations as a function of reaction time in He and O_2 only. The open symbols are the measured OH concentrations for the same system with NO added. The overall reaction times were estimated from the distance between the injection of α-pinene to the OH detection axis and corrected to account for the decrease in the effective velocity as the gas enters the larger diameter detection chamber. This correction added approximately 2 ms to the reaction time based on distance alone. The lines through these data points are computer simulations of the OH concentration profiles for the various reactant concentrations. As can be seen from this figure, the OH concentration profiles were limited by the concentration of NO, as the OH concentration increased with increasing NO concentration.

Table 2
Rate constants used in the model for the OH-initiated oxidation of α-pinene

Reaction	Reaction code	Rate constants (300 K)[a]	Reference
$OH + PINENE \xrightarrow{O_2} RO_2$	k_a	6.09×10^{-11}	This work
$RO_2 + NO \rightarrow \gamma RNO_3 + (1-\gamma)RO + NO_2$	k_b[b]	8.43×10^{-12}	MCM
$RO \xrightarrow{O_2}$ aldehyde or ketone $+ XO_2$ (e.g. APINAO $\xrightarrow{O_2}$ pinonaldehyde $+ HO_2$)	k_c	$1 \times 10^6\ s^{-1}$	MCM
$RCO + O_2 \rightarrow$ carbonyl $+ HO_2$	k_d	7.57×10^{-15}	MCM
Pinonaldehyde $+ OH \rightarrow$ products	k_e	4.2×10^{-11}	MCM
$RO \xrightarrow{O_2}$ products (isomerization) (abstraction of H from 1° carbon attached to a 3° carbon)	k_f	$2 \times 10^5\ s^{-1}$	(Atkinson, 1997)
$RO \xrightarrow{O_2}$ products (isomerization) (abstraction of H from 2° carbon attached to two 3° carbon)	k_g	$2.6 \times 10^6\ s^{-1}$	(Atkinson, 1997)
$RO \xrightarrow{O_2}$ products (isomerization) (abstraction of H from 3° carbon attached to a 3° carbon, a 2° carbon, and an OH)	k_h	$2.7 \times 10^7\ s^{-1}$	(Atkinson, 1997)

[a]All rate constants are in units of $cm^3\ molecule^{-1}\ s^{-1}$ except where otherwise stated.
[b]The values of γ are indicated in Fig. 3.

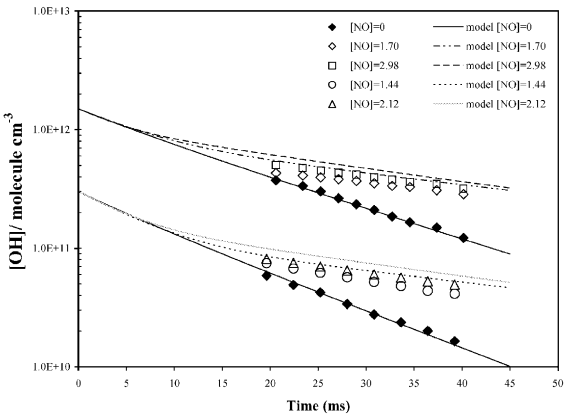

Fig. 4. Observed and simulated OH radical propagation results for the OH + α-pinene + O_2 + NO reaction system using the MCM mechanism for the simulation. NO concentrations are in units of 10^{13} molecule cm^{-3}. The upper set of data is offset by a factor of 5 for clarity. For the upper set of data, [α-pinene] $= 1.0 \times 10^{12}$ molecule cm^{-3}, $[O_2] = 2.5 \times 10^{15}$ molecule cm^{-3}. For the lower data set, [α-pinene] $= 1.4 \times 10^{12}$ molecule cm^{-3}, $[O_2] = 5.5 \times 10^{15}$ molecule cm^{-3}.

4. Discussion

As can be seen from Fig. 4, the modeled OH radical propagation based on the MCM mechanism is in reasonable agreement with the observed OH concentration profiles using a value of 8.4×10^{-12} $cm^3\ molecule^{-1}\ s^{-1}$ for the reaction of α-pinene-based peroxy radicals with NO (with an organic nitrate yield of 23%), although the model generally overpredicts the observations by 10–30%. This agreement between observations and the MCM model predictions is consistent with the results of Saunders et al. (2003) using photochemical chamber experiments to assist in the validation of the MCM model. The oxidation of α-pinene/NO_x mixtures were studied over 4–6 h under conditions in which the oxidations were driven primarily by the reaction with the OH radical. The concentrations of α-pinene, NO, NO_2, and O_3 were measured and compared to their respective predicted levels. They found that initially (for reaction times less than 1 h) there was excellent agreement between the observed and predicted concentrations for all entities measured. For reaction times greater than 1 h, the predicted NO_2 concentration was significantly less than the observed concentration. This was attributed to interferences associated with the measurement technique, although the modeled ozone concentrations were also less than the observed.

The MCM model assumes that the sole fate of the alkoxy radicals is decomposition. However, isomerization of the alkoxy radicals via a 1–5 H-shift or a 1–6 H-shift have been suggested based on product studies and theoretical calculations (Aschmann et al., 2002; Atkinson and Arey, 1998, 2003; Dibble, 2001), although the barrier to isomerization through this strained transition state would have to be quite low to compete with ring opening (Peeters et al., 2001). These pathways are shown in Fig. 3 enclosed in the box and with dashed arrows. The alkyl radicals formed from the isomerization promptly form peroxy radicals whose reaction with NO to form alkoxy radicals lead to the formation of

dihydroxy carbonyl compounds, some of which have been identified as having molecular weight of 184 (Aschmann et al., 2002). Based on these results, it is possible that decomposition is not the only available reaction channel for these alkoxy radicals.

The branching ratio between decomposition and isomerization of these alkoxy radicals influences the overall pinonaldehyde yield and directly affects the rate of radical propagation, as HO_2 production in the proposed isomerization channel occurs after a second NO oxidation step, while decomposition leading to the formation of pinonaldehyde leads directly to HO_2 production. In addition, a portion of radicals produced through the proposed isomerization channel is terminated from the cycle through the formation of organic nitrates. To determine the effect of this channel on the modeled OH concentration profiles, these reaction paths were added to the simulation, with rates based on recommended rate constants for the isomerization of alkoxy radicals by Atkinson (1997) (Table 2). Based on these rules, values of 2×10^5, 2.6×10^6, and $2.7\times10^7\,s^{-1}$ were obtained for the isomerization rate constants k_f, k_g, and k_h, respectively, and are within the range of values expected for alkoxy radical isomerizations (Orlando et al., 2003). When this isomerization channel is added to the model, the OH concentration profiles are reduced by approximately 10–20%, and the agreement between the predicted and measured OH concentration is improved (Fig. 5), with predicted OH concentrations within 10% of the measured values on average. The modeled pinonaldehyde yield with the isomerization channel included is reduced to 45%.

The observed OH profiles were also compared to that predicted by the treatment of α-pinene chemistry by the Regional Atmospheric Chemistry Mechanism (RACM) discussed in detail by Stockwell et al. (1997):

$$\mathrm{OH} + \alpha\text{-pinene} \rightarrow \mathrm{APIP}$$

$$\mathrm{APIP} + \mathrm{NO} \rightarrow 0.80\,\mathrm{HO_2} + 0.80\ (\mathrm{C2-C4\ aldehydes})$$

$$+ 0.80\ \mathrm{ketone} + 0.80\ \mathrm{NO_2} + 0.20\ \mathrm{RONO_2}$$

$$k = 4\times10^{-12}\,\mathrm{cm^3\,molecule^{-1}\,s^{-1}} \qquad \text{(R9)}$$

Subsequent OH reactions with aldehydes and ketones in addition to peroxy radical reactions were included in this mechanism. The results of the simulation are shown in Fig. 5. As seen in this figure, the RACM mechanism for the OH-initiated oxidation of α-pinene reproduces the observed OH concentration profiles reasonably well, although it tends to overestimate the OH concentrations at longer reaction times.

The RACM mechanism assumes a 20% organic nitrate formation yield but uses a rate constant of

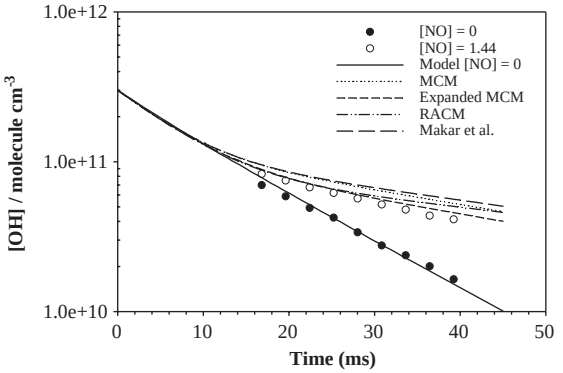

Fig. 5. Observed and simulated OH radical propagation results for the OH + α-pinene + O_2 + NO reaction system showing the difference between the results obtained using the MCM, the expanded MCM, RACM and Makar et al. models. NO concentrations are in units of 10^{13} molecule cm^{-3}. [α-pinene] = 1.4×10^{12} molecule cm^{-3}, [O_2] = 5.5×10^{15} molecule cm^{-3}.

$4\times10^{-12}\,\mathrm{cm^3\,molecule^{-1}\,s^{-1}}$ for the reaction of the peroxy radicals with NO, lower than the recommended value of $9\times10^{-12}\,\mathrm{cm^3\,molecule^{-1}\,s^{-1}}$ for RO_2 + NO reactions (Atkinson et al., 1999), and the value of $8.4\times10^{-12}\,\mathrm{cm^3\,molecule^{-1}\,s^{-1}}$ used in the MCM mechanism. The reduction of this rate constant appears to compensate for the prompt formation of HO_2 radicals in the condensed mechanism compared to the expanded MCM mechanism, where a significant fraction of HO_2 is produced after a second NO oxidation step through the isomerization channels. Using the recommended rate constant for RO_2 + NO reactions of 9×10^{-12} $\mathrm{cm^3\,molecule^{-1}\,s^{-1}}$ the RACM model overestimates the observed OH concentrations by approximately 30%, consistent with the MCM mechanism without isomerization. Similar results are obtained using other condensed models of α-pinene oxidation, such as that proposed by Makar et al. (1999) which assumes a rate constant of $7.6\times10^{-12}\,\mathrm{cm^3\,molecule^{-1}\,s^{-1}}$ and an organic nitrate yield of 30% for the RO_2 + NO reaction in a mechanism similar to the RACM mechanism described above. These results suggest that condensed mechanisms using a rate constant of $8–9\times10^{-12}$ $\mathrm{cm^3\,molecule^{-1}\,s^{-1}}$ for the RO_2 + NO reaction may overestimate the efficiency of OH radical cycling by α-pinene.

Although these experiments suggest that the MCM and RACM chemical mechanisms for α-pinene oxidation are able to simulate radical cycling in the atmosphere well, there are several potential sources of error in these radical propagation experiments. The low-pressure conditions of these experiments bring into question the applicability of these measurements to atmospheric conditions, as the reaction rates and mechanism of

radical propagation may be different at low pressure. There are a few studies that suggest that the alkyl nitrate yield from the oxidation of C_5–C_8 *n*-alkanes depends strongly on pressure (Atkinson et al., 1983, 1987; Arey et al., 2001). Reducing the organic nitrate yield by a factor of 3 in these simulations would increase the modeled OH concentration profiles by approximately 20%. However, recent master equation modeling studies of alkyl nitrate yields have shown that as the value of the average energy transferred in deactivating collisions is increased, the modeled yield becomes less and less dependent on pressure (Barker et al., 2003). Due to the greater number of vibrational degrees of freedom in the α-pinene system, it is possible that the organic nitrate yield as well as the majority of the channels in the α-pinene oxidation mechanism may be at their high pressure limits even under the low-pressure conditions of these experiments. Clearly, additional measurements at higher pressures are needed to confirm these results.

Although the majority of the channels in the α-pinene oxidation mechanism are likely to be independent of pressure, the branching ratio between stabilization and ring breaking of the chemically activated C2 alkyl radical may be different at low pressure compared to atmospheric conditions, resulting in a larger contribution of the APINCO2 channel to the overall acetone yield (Vereecken and Peeters, 2000). This may affect the propagation of radicals in these experiments, as this channel leads to the production of HO_2 after a second $RO_2 + NO$ oxidation step. However, a sensitivity analysis of the impact of this channel on the modeled regeneration of OH suggests that an increase of the contribution of this channel by a factor of 3 (reflecting a calculated acetone yield of approximately 20%) reduces the calculated OH concentrations by less than 10%. As a result, the impact of the pressure dependence of this channel on the efficiency of radical propagation is small under the conditions of these experiments.

In addition, the rates of isomerization and decomposition of the various thermally stabilized alkyl and alkoxy radicals may be slower than at atmospheric pressure, and the rates of these reactions relative to reaction with molecular oxygen may be significantly different under the low-pressure conditions of these experiments (Reitz et al., 2002). Nevertheless, since these experiments were conducted under conditions where the regeneration of OH radicals was limited by the concentration of NO, the rates of isomerization and decomposition of the various alkoxy radicals are not limiting the rate of radical propagation. As a result, the model results are not sensitive to these rates over several orders of magnitude. In addition, the measured OH concentration profiles in these experiments were independent of the concentration of O_2 over a factor of 10, which suggests that the rate of radical propagation was not limited by reactions of O_2 in the chemical mechanism.

Peeters et al. (2001) have suggested that the formation of pinonaldehyde in the α-pinene oxidation mechanism is the result of decomposition of α-hydroxyalkyl peroxy radicals formed from the reaction of α-hydroxyalkyl radicals with O_2, citing evidence that α-hydroxyalkyl + O_2 reactions are not direct abstractions but proceed through an activated peroxy radical intermediate that could be conditionally stabilized:

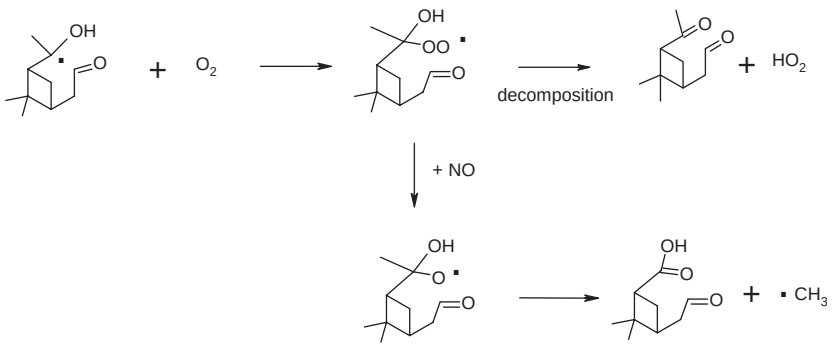

Under atmospheric conditions, the rate of decomposition of these stabilized α-hydroxyalkyl peroxy radicals to form pinonaldehyde and HO_2 should be greater than the rate of reaction with NO, and thus dominate the fate of these radicals. However, under laboratory conditions with NO concentrations in the order of $(2–20) \times 10^{14}\,cm^{-3}$, the reaction of these stabilized α-hydroxyalkyl peroxy radicals with NO may compete with decomposition. This could lead to a different mechanism and product yield under laboratory NO conditions compared to atmospheric conditions. However, because of the relatively low concentrations of NO used in these experiments ($1–2 \times 10^{13}\,cm^{-3}$), the rate of decomposition of these α-hydroxyalkyl peroxy is likely to be faster than reaction with NO. As a result,

these radical propagation results likely reflect atmospheric rather than the laboratory conditions described in Peeters et al. (2001).

Another source of error is the existence of secondary radical termination reactions not included in the chemical model, such as unknown radical losses to the walls of the flow tube. A first-order loss rate of $10\,s^{-1}$ was assumed for the heterogeneous reaction of peroxy radicals in these simulations, similar to that observed for OH radicals. Future experiments will involve measurement at higher pressures using turbulent flow techniques to reduce this uncertainty, in addition to reducing any uncertainties associated with the pressure dependence of the oxidation mechanism.

5. Conclusion

These measurements of the OH-initiated oxidation of α-pinene suggest that the efficiency of radical propagation reactions in the presence of NO is consistent with current models of α-pinene oxidation. The observed OH radical propagation was compared to predictions based on the near-explicit Master Chemical Mechanism (MCM) and the condensed Regional Atmospheric Chemistry Mechanism (RACM). Both models simulate the propagation of radicals reasonably well within the uncertainties of these experiments. Expanding the MCM to include isomerization of the β-hydroxy alkoxy radicals results in a reduction in the simulated propagation of radicals of approximately 10–20% and improves the agreement with the experimental OH concentration profiles.

The RACM model was able to reproduce the observed OH concentration profile reasonably well using a reduced rate constant for the $RO_2 + NO$ reaction. The reduction of this rate constant may compensate for the prompt formation of HO_2 in the condensed mechanism compared to the explicit mechanism, where radical isomerization channels lead to the slower production of HO_2 after a second $RO_2 + NO$ oxidation step. Condensed mechanisms that use a larger value for this reaction step may overestimate the rate of radical propagation by α-pinene in the atmosphere. Further experiments under conditions at higher pressures where unknown radical losses are minimized in addition to reducing the uncertainties in the pressure dependence of the oxidation mechanism are needed to confirm these results.

Acknowledgements

This work was supported by a grant from the National Science Foundation (ATM-0106705).

References

Arey, J., Atkinson, R., Aschmann, S.M., 1990. Product study of the gas-phase reactions of monoterpenes with the OH radical in the presence of NO_x. Journal of Geophysical Research—Atmospheres 95, 18539–18546.

Arey, J., Aschmann, S.M., Kwok, E.S.C., Atkinson, R., 2001. Alkyl nitrate, hydroxyalkyl nitrate, and hydroxycarbonyl formation from the NO_x–air photooxidation of C_5–C_8 *n*-alkanes. Journal of Physical Chemistry A 105, 1020–1027.

Aschmann, S.M., Atkinson, R., Arey, J., 2002. Products of reaction of OH radicals with α-pinene. Journal of Geophysical Research—Atmospheres 107, 10.1029/2001JD001098.

Atkinson, R., 1994. Gas-phase tropospheric chemistry of organic compounds. Journal of Physical and Chemical Reference Data Monograph 2, R1.

Atkinson, R., 1997. Atmospheric reactions of alkoxy and β-hydroxyalkoxy radicals. International Journal of Chemical Kinetics 29, 99–111.

Atkinson, R., 2000. Atmospheric chemistry of VOCs and NO_x. Atmospheric Environment 34, 2063–2101.

Atkinson, R., Arey, J., 1998. Atmospheric chemistry of biogenic organic compounds. Accounts of Chemical Research 31, 574–583.

Atkinson, R., Arey, J., 2003. Gas-phase tropospheric chemistry of biogenic volatile organic compounds: a review. Atmospheric Environment 37 (Suppl. 2), 197–219.

Atkinson, R., Carter, W.P.L., Winer, A.M., 1983. Effects of temperature and pressure on alkyl nitrate yields in the NO_x photooxidations of *n*-pentane and *n*-heptane. Journal of Physical Chemistry 87, 2012–2018.

Atkinson, R., Aschmann, S.M., Pitts, J.N., 1986. Rate constants for the gas-phase reactions of the OH radical with a series of monoterpenes at 294 ± 1 K. International Journal of Chemical Kinetics 18, 287–299.

Atkinson, R., Aschmann, S.M., Winer, A.M., 1987. Alkyl nitrate formation from the reaction of a series of branched RO2 radicals with NO as a function of temperature and pressure. Journal of Atmospheric Chemistry 5, 91–102.

Atkinson, R., et al., 1999. Evaluated kinetic and photochemical data for atmospheric chemistry, organic species: Supplement VII. Journal of Physical and Chemical Reference Data 28, 191–393.

Barker, J.R., Lohr, L.L., Shroll, R.M., Reading, S., 2003. Modeling the organic nitrate yields in the reaction of alkyl peroxy radicals with nitric oxide. 2. Reaction simulations. Journal of Physical Chemistry A 107, 7434–7444.

Bedjanian, Y., Laverdet, G., Le Bras, G., 1998. Low-pressure study of the reaction of Cl atoms with isoprene. Journal of Physical Chemistry A 102, 953–959.

Carslaw, N., et al., 1999. Modeling OH, HO_2, and RO_2 radicals in the marine boundary layer—1. Model construction and comparison with fiels measurements. Journal of Geophysical Research 104, 30241–30255.

Chuong, B., Stevens, P.S., 2000. Kinetic study of the OH + isoprene and OH + ethylene reactions between 2 and 6 torr and over the temperature range 300–423 K. Journal of Physical Chemistry A 104, 5230–5237.

Chuong, B., Stevens, P.S., 2003. Kinetics of the OH + methyl vinyl ketone and OH + methacrolein reactions at low pressure. Journal of Physical Chemistry A 107, 2185–2191.

Chuong, B., Davis, M., Edwards, M., Stevens, P.S., 2002. Measurements of the kinetics of the OH + α-pinene and OH + β-pinene reactions at low pressure. International Journal of Chemical Kinetics 34, 300–308.

Dibble, T.S., 2001. Reactions of the alkoxy radicals formed following OH-addition to α-pinene and β-pinene. C–C bond scission reactions. Journal of the American Chemical Society 123, 4228–4234.

George, L.A., Hard, T.M., O'Brien, R.J., 1999. Measurement of free radicals OH and HO_2 in Los Angeles smog. Journal of Geophysical Research 104, 11643–11655.

Gill, K.J., Hites, R.A., 2002. Rate constants for the gas-phase reactions of the hydroxyl radical with isoprene, α- and β-pinene, and limonene as a function of temperature. Journal of Physical Chemistry A 106, 2538–2544.

Guenther, A., et al., 1995. A global model of natural volatile organic compound emissions. Journal of Geophysical Research 100, 8873–8892.

Guenther, A., et al., 2000. Natural emissions of non-methane volatile organic compounds; carbon monoxide, and oxides of nitrogen from North America. Atmospheric Environment 34, 2205–2230.

Hakola, H., Arey, J., Aschmann, S.M., Atkinson, R., 1994. Product formation from the gas-phase reactions of OH radicals and O_3 with a series of monoterpenes. Journal of Atmospheric Chemistry 18, 75–102.

Hatakeyama, S., Izumi, K., Fukuyama, T., Akimoto, H., Washida, N., 1991. Reactions of OH with α-pinene and β-pinene in air—estimate of global CO production from the atmospheric oxidation of terpenes. Journal of Geophysical Research 96, 947–958.

Howard, C.J., 1979. Kinetic measurements using flow tubes. Journal of Physical Chemistry 83, 3–9.

Ianni, J.C., Bandy, A.R., 2000. A theoretical study of the hydrates of $(H_2SO_4)_2$ and its implications for the formation of new atmospheric particles. Journal of Molecular Structure: THEOCHEM 497, 19–37.

Kleindienst, T.E., Harris, G.W., Pitts, J.N., 1982. Rates and temperature dependences of the reaction of OH with isoprene, its oxidation products, and selected terpenes. Environmental Science and Technology 16, 844–846.

Larsen, B.R., et al., 2001. Gas-phase OH oxidation of monoterpenes: gaseous and particulate products. Journal of Atmospheric Chemistry 38, 231–276.

Makar, P.A., Fuentes, J.D., Wang, D., Staebler, R.M., Wiebe, H.A., 1999. Chemical processing of biogenic hydrocarbons within and above a temperate deciduous forest. Journal of Geophysical Research—Atmospheres 104, 3581–3603.

McKeen, S.A., et al., 1997. Photochemical modeling of hydroxyl and its relationship to other species during the Tropospheric OH Photochemistry Experiment. Journal of Geophysical Research 102, 6467–6493.

Noziere, B., Barnes, I., Becker, K.H., 1999. Product study and mechanisms of the reactions of α-pinene and of pinonaldehyde with OH radicals. Journal of Geophysical Research 104, 23645–23656.

Orlando, J.J., et al., 2000. Product studies of the OH- and ozone-initiated oxidation of some monoterpenes. Journal of Geophysical Research—Atmospheres 105, 11561–11572.

Orlando, J.J., Tyndall, G.S., Wallington, T.J., 2003. The atmospheric chemistry of alkoxy radicals. Chemical Reviews 103, 4657–4689.

Peeters, J., Vereecken, L., Fantechi, G., 2001. The detailed mechanism of the OH-initiated atmospheric oxidation of α-pinene: a theoretical study. Physical Chemistry Chemical Physics 3, 5489–5504.

Reitz, J.E., McGivern, W.S., Church, M.C., Wilson, M.D., North, S.W., 2002. The fate of the hydroxyalkoxy radical in the OH-initiated oxidation of isoprene. International Journal of Chemical Kinetics 34, 255–261.

Saunders, S.M., Jenkin, M.E., Derwent, R.G., Pilling, M.J., 2003. Protocol for the development of the Master Chemical Mechanism, MCM v3 (Part A): tropospheric degradation of non-aromatic volatile organic compounds. Atmospheric Chemistry and Physics 3, 161–180.

Stevens, P., L'Esperance, D., Chuong, B., Martin, G., 1999. Measurements of the kinetics of the OH-initiated oxidation of isoprene: radical propagation in the OH + isoprene + O_2 + NO reaction system. International Journal of Chemical Kinetics 31, 637–643.

Stevens, P.S., et al., 1997. HO_2/OH and RO_2/HO_2 ratios during the Tropospheric OH Photochemistry Experiment: measurement and theory. Journal of Geophysical Research 102, 6379–6391.

Stockwell, W.R., Kirchner, F., Kuhn, M., Seefeld, S., 1997. A new mechanism for regional atmospheric chemistry modeling. Journal of Geophysical Research 102, 25847–25879.

Stutz, J., Ezell, M.J., Ezell, A.A., Finlayson-Pitts, B.J., 1998. Rate constants and kinetic isotope effects in the reactions of atomic chlorine with *n*-butane and simple alkenes at room temperature. Journal of Physical Chemistry A 102, 8510–8519.

Tan, D., et al., 2001. HO_x budgets in a deciduous forest: results from the PROPHET summer 1998 campaign. Journal of Geophysical Research 106, 24407–24427.

Vereecken, L., Peeters, J., 2000. Theoretical study of the formation of acetone in the OH-initiated atmospheric oxidation of α-pinene. Journal of Physical Chemistry A 104, 11140–11146.

Winer, A.M., Lloyd, A.C., Darnall, K.R., Pitts Jr., J.N., 1976. Relative rate constants for the reaction of the hydroxyl radical with selected ketones, chloroethenes, and monoterpene hydrocarbons. Journal of Physical Chemistry 80, 1635–1639.

Wisthaler, A., Jensen, N.R., Winterhalter, R., Lindinger, W., Hjorth, J., 2001. Measurements of acetone and other gas phase product yields from the OH-initiated oxidation of terpenes by proton-transfer-reaction mass spectrometry (PTR-MS). Atmospheric Environment 35, 6181–6191.